Supporting Information

Sigala et al. 10.1073/pnas.0900168106

SI Text

Discussion of NMR Spectra of Glu46Gln and Tyr42Phe Mutants

Glu46Gln. A single downfield peak at 15.2 ppm is observed in the Glu46Gln spectrum, as expected for the single short Tyr-42·chromophore hydrogen bond (2.50 Å O···O distance) observed in the 0.95 Å resolution X-ray structure of Glu46Gln (1). Two models can account for the identical chemical shift of the 15.2 ppm peak in Glu46Gln and the 15.2 ppm peak observed in the WT spectrum (Fig. 2).

Model #1: The Peaks Observed at 15.2 ppm in the Glu46Gln and WT Spectra both Arise from the Tyr-42 Hydrogen Bond, Whose Structure Is Unaltered by the Glu46Gln Mutation. This model is consistent with ultra-high resolution X-ray structures of WT (0.82 Å) and Glu46Gln (0.95 Å) that refined identical O···O distances for the Tyr-42·chromophore hydrogen bond of 2.48 Å (1, 2). This model is inconsistent with the following observations discussed in the text: (*i*) A high resolution neutron structure of PYP identified a significantly longer O-D bond for Glu-46 (1.20 Å) than for Tyr-42 (0.96 Å), directly suggesting a more downfield chemical shift for the Glu-46 hydrogen-bonded proton relative to Tyr-42; (*ii*) A strong NOE was detected from the 13.7 ppm peak but not the 15.2 ppm peak to Tyr-42 ring protons in a NOESY spectrum of WT PYP; and (*iii*) H/D substitution studies identified strong physical coupling between the Tyr-42 and Glu-46 hydrogen bonds (with lengthening of one via deuteration resulting in a shortening of the neighbor), suggesting that mutation of 1 hydrogen bond perturbs the bond lengths of the coupled neighbor.

Model #2: The 15.2 ppm Peak Arises from the Glu-46 Hydrogen Bond in WT but Is Due to the Tyr-42 Hydrogen Bond in Glu46Gln. This model posits that the chemical shift of the Tyr-42 hydrogen bonded proton increases from 13.7 ppm in WT to 15.2 ppm in Glu46Gln, as expected if the Tyr-42 O-H bond lengthens in response to the Glu46Gln mutation to move the bridging proton closer to the chromophore oxygen that accepts a hydrogen bond from it. This model is consistent with the observations described above for the neutron structure of WT PYP, NOESY spectrum of WT, and H/D substitution studies of Tyr-42 and Glu-46 that provide strong evidence for hydrogen bond coupling. In the case of the Tyr42Phe mutant (see Fig. 2 and below), there is a change in the chemical shift of the remaining hydrogen bond peak. This change is in agreement with the detected coupling from the H/D substitution studies (described extensively in the text). Thus, the default expectation upon mutagenesis of one hydrogen bond donor is a change in the chemical shift of the remaining donor, rather than an absence of an effect.

For Tyr-42, X-ray structures of WT and Glu46Gln give nearly identical 2.5 Å O···O distances for its hydrogen bond, despite the expectation from small molecules that a change in O-H distance is accompanied by a change in O···O distance. However, the lack of O···O distance change is consistent with the structural constraints on the relative positions of the Tyr-42 and chromophore oxygens preventing such change, as discussed above and in the text. Presumably the Tyr-42 O-H bond still lengthens in response to the Glu46Gln mutation, resulting in the observed chemical shift change, even if there is no detectable change in the O···O distance.

Model #2, but not Model #1, is consistent with the above observations. Thus, in the spectrum of WT PYP, we assign the 15.2 ppm peak to Glu-46 and the 13.7 ppm peak to Tyr-42 according to Model #2.

Tyr42Phe. A single peak is detected at 16.7 ppm in the Tyr42Phe spectrum, shifted 1.5 ppm downfield from the peak assigned to Glu-46 in the WT spectrum (see above). This chemical shift change suggests increased migration of the Glu-46 hydroxyl proton toward the chromophore oxygen in response to the Tyr42Phe mutation. Such proton migration is most simply expected to be accompanied by a shortening of the Glu-46·chromophore O···O distance. Such shortening was indeed reported in a 1.10 Å resolution structure of Tyr42Phe that identified an O···O distance of 2.51 Å for the Glu-46·chromophore hydrogen bond relative to its 2.59 Å distance observed in a 0.82 Å resolution WT structure (3). The broad NMR line-width observed for the Tyr42Phe mutant is consistent with UV/VIS, FT Raman, and fluorescence spectroscopy studies of this mutant that suggested the presence of 2 structurally similar and interconverting chromophore conformations (3).

SI Materials and Methods

Materials. All reagents were of the highest purity commercially available. Substituted phenols, *p*-coumaric acid (pCA), cyano-*p*-coumaric acid (pCA-CN), carbonyl diimidazole (CDI), and bovine thrombin were purchased from Sigma. All buffers were prepared with reagent-grade chemicals or better.

PYP Mutagenesis. A plasmid encoding PYP from *H. halophila* inserted between the *Nde*I and *Bam*H1 sites of the pET15b vector was a gift from Elizabeth Getzoff (Scripps Research Institute, La Jolla, CA). QuikChange site-directed mutagenesis was used to introduce the Tyr42Phe, Glu46Gln, and Thr50Val mutations, which were confirmed by sequencing miniprep DNA from DH5α cells on an ABI3100 capillary sequencer.

PYP Expression, Reconstitution, and Purification

Protein Expression. Apo PYP containing an N-terminal hexahistidine tag and thrombin cleavage site was expressed from *E. coli* BL21(DE3) cells transformed with the pET15b plasmid encoding PYP. A 20-mL overnight culture of the transformed cells was diluted into 2 L LB supplemented with 50 μg/mL carbenicillin and grown at 37 °C for 3 h to an OD of 0.4. Protein expression was induced by addition of 0.5 mM IPTG (final concentration), and cells were grown for an additional 4 h. Cells were harvested by centrifugation (4000 rpm for 20 min), resuspended in 30 mL 40 mM potassium phosphate (KP_i) buffer, pH 7.5, and lysed by passage through a French pressure cell. Lysates were centrifuged (20,000 rpm for 20 min) to pellet insoluble cellular debris.

For production of ^{15}N-labeled PYP, the 20-mL overnight culture was diluted into 2 L M9 minimal medium (4) containing $^{15}NH_4Cl$ as the sole nitrogen source during protein expression.

Chromophore Attachment. For reconstitution of native PYP or PYP-CN, chromophores were activated for attachment to apo PYP by dissolving 58 mg pCA and 64 mg CDI in 8 mL anhydrous THF or 60 mg pCA-CN and 64 mg CDI in 1 mL anhydrous DMF in a round bottom flask. Reactions were stirred under Ar for 45 min. Solvent was removed by rotary evaporation, and the resultant paste was resuspended in 5 mL water and added to the clarified cell lysate supernatant. This mixture turned deep yellow within minutes and was stirred for 1 h at room temperature on an orbital shaker. The mixture was centrifuged (20,000 rpm for

20 min), and the supernatant was passed through a 0.2-μm syringe filter.

Protein Purification. The clarified solution of crude PYP (apo or chromophore reconstituted) was passed manually over a 5-mL HiTrap Chelating column that had been preloaded with Ni^{2+} and equilibrated with buffer containing 40 mM KP_i, pH 7.5, 0.5 M NaCl, and 5 mM imidazole (buffer A). The loaded column was connected to an FPLC and washed with 20 column volumes of buffer A. PYP was eluted from the column using a linear gradient over 5 column volumes of buffer A to buffer B (buffer A supplemented with 0.5 M imidazole). Visibly yellow fractions (or protein-containing fractions for apo PYP) were pooled and concentrated to approximately 6 mL with Amicon spin concentrators. Cleavage of the N-terminal His-tag (which leaves Gly-Ser-His on the N terminus of the cleaved PYP) was carried out by adding 1 mg bovine thrombin to the 6-mL solution and incubating at room temperature for 2 h on a rotary shaker. The solution was then passed through a 0.2-μm syringe filter and further purified by injection over a 100-mL superose-12 gel filtration column in 40 mM KP_i, pH 7.2, 1 mM EDTA buffer. Protein-containing fractions were pooled and concentrated to approximately 1 mL using Amicon spin concentrators. Typical yields were 30–40 mg protein from a 2-L culture. Protein concentrations were determined by absorbance at 446 nm for PYP, 466 nm for PYP-CN, and 280 nm for apo PYP using molar extinction coefficients of 42,000 $M^{-1}cm^{-1}$ for PYP, 55,000 $M^{-1}cm^{-1}$ for PYP-CN, and 12,950 $M^{-1}cm^{-1}$ for apo PYP (5). Optical purities of PYP (A_{280}/A_{446}) and PYP-CN (A_{280}/A_{466}) were typically <0.5 and <0.4, respectively. Protein purity was confirmed by the appearance of a single band on an overloaded SDS/PAGE gel. Protein masses were confirmed by LCMS and were within 5 Da of the expected values.

NMR Spectroscopy. ^1H NMR spectra of PYP were acquired at the Stanford Magnetic Resonance Laboratory on an 800-MHz Varian ^{UNITY}INOVA spectrometer running VNMR v6.1C and equipped with a 5-mm, triple resonance, gradient $^1H(^{13}C/^{15}N)$ probe. NMR samples consisted of 0.5 mM PYP (and 3.0 mM substituted phenol for apo PYP·phenolate complexes) in 40 mM KP_i buffer (pH 7.2), 1 mM EDTA, and 5%–75% (vol/vol) D_2O in 5 mm Shigemi symmetrical microtubes at 4.0° ± 0.5 °C.

One-dimensional proton spectra were acquired using the 1331 binomial pulse sequence (6) to suppress the water signal, with a spectral width of 30 ppm (carrier frequency set on the water resonance) and an excitation maximum of 15 ppm. Data were collected with 32,000 points and a 1.9 s recycle delay for 512–5120 scans and processed using a 10-Hz line broadening, with a baseline correction applied over the peaks of interest. Chemical shifts were referenced internally to the water resonance (4.6 ppm at 4 °C) and externally to a sample of sodium-3-trimethylsilylpropionate-2,2,3,3-d_4 (0 ppm) in the same buffer conditions. Spectral deconvolution of overlapping peaks was carried out using the ACD/NMR Processor software. Hydrogen bond distances were estimated from the observed chemical shifts for the detected hydrogen-bonded protons using references (7) and (8) and the following correlation functions:

a. O···O distance (Å) = 5.040 Å − 1.160*ln(chemical shift) + 0.044*(chemical shift)
b. H···O-acceptor distance (Å) = 2.380 Å − 0.055*(chemical shift)

Two-dimensional ^1H-^1H NOESY spectra were acquired using the SS-NOESY pulse sequence to minimize saturation of protons exchanging with bulk water (9). Data were acquired over 23.8 ppm spectral widths of 2048 data points with a 50-ms mixing time, 1.55-s recycle delay, and 64 scans per t_1 increment over 256 increments. Spectra were processed using shifted, squared sine bell window functions in both dimensions and one-fold zero filling in the t_1 dimension and viewed with the program SPARKY (10).

Two-dimensional ^1H-^{15}N HSQC spectra of ^{15}N-labeled PYP, PYP-CN, and apo PYP·3-F-4-nitrophenolate were acquired at 25 °C on a 600-MHz Varian ^{UNITY}INOVA spectrometer running VNMR v6.1C and equipped with a 5-mm, triple resonance, gradient $^1H(^{13}C/^{15}N)$ probe. Spectra were viewed with the program SPARKY.

UV Absorbance Spectroscopy. Absorbance spectra for PYP and PYP-CN were acquired in a microcuvet with a Uvikon 9310 absorbance spectrophotometer. Binding of 5 μM 4-nitrophenolate to apo PYP was monitored by the increase in absorbance at 398 nm as the concentration of apo PYP was increased from 0 to 480 μM. The observed absorbance values at each concentration of apo PYP were fit to a quadratic binding equation (11) to determine an apparent dissociation constant (K_d) for 4-nitrophenolate binding of 30 μM. pK_a values for the phenolic hydroxyl of pCA and pCA-CN were determined by spectral titration (12) at the absorbance maxima for the phenolate forms at 25 °C and an ionic strength of 100 mM, maintained with NaCl.

1. Anderson S, Crosson S, Moffat K (2004) Short hydrogen bonds in photoactive yellow protein. *Acta Crystallogr D* 60:1008–1016.
2. Getzoff ED, Gutwin KN, Genick UK (2003) Anticipatory active-site motions and chromophore distortion prime photoreceptor PYP for light activation. *Nat Struct Biol* 10:663–668.
3. Brudler R, et al. (2000) Coupling of hydrogen bonding to chromophore conformation and function in photoactive yellow protein. *Biochemistry* 39:13478–13486.
4. Marley J, Lu M, Bracken C (2001) A method for efficient isotopic labeling of recombinant proteins. *J Biomol NMR* 20:71–75.
5. Gill SC, von Hippel PH (1989) Calculation of protein extinction coefficients from amino acid sequence data. *Anal Biochem* 182:319–326.
6. Turner DL (1983) Binomial solvent suppression. *J Magn Reson* 54:146–148.
7. Jeffrey GA, Yeon Y (1986) The correlation between hydrogen-bond lengths and proton chemical shifts in crystals. *Acta Crystallogr B* 42:410–413.
8. Harris TK, Mildvan AS (1999) High-precision measurement of hydrogen bond lengths in proteins by nuclear magnetic resonance methods. *Proteins* 35:275–282.
9. Smallcombe SH (1993) Solvent suppression with symmetrically-shifted pulses. *J Am Chem Soc* 115:4776–4785.
10. SPARKY, Goddard TD, Kneller DG (2004) (University of California, San Francisco).
11. Kraut DA, et al. (2006) Testing electrostatic complementarity in enzyme catalysis: Hydrogen bonding in the ketosteroid isomerase oxyanion hole. *PLoS Biol* 4:e99.
12. Petrounia IP, Blotny G, Pollack RM (2000) Binding of 2-naphthols to D38E mutants of 3-oxo-delta 5-steroid isomerase: Variation of ligand ionization state with the nature of the electrophilic component. *Biochemistry* 39:110.
13. Dux P, et al. (1998) Solution structure and backbone dynamics of the photoactive yellow protein. *Biochemistry* 37:12689–12699.

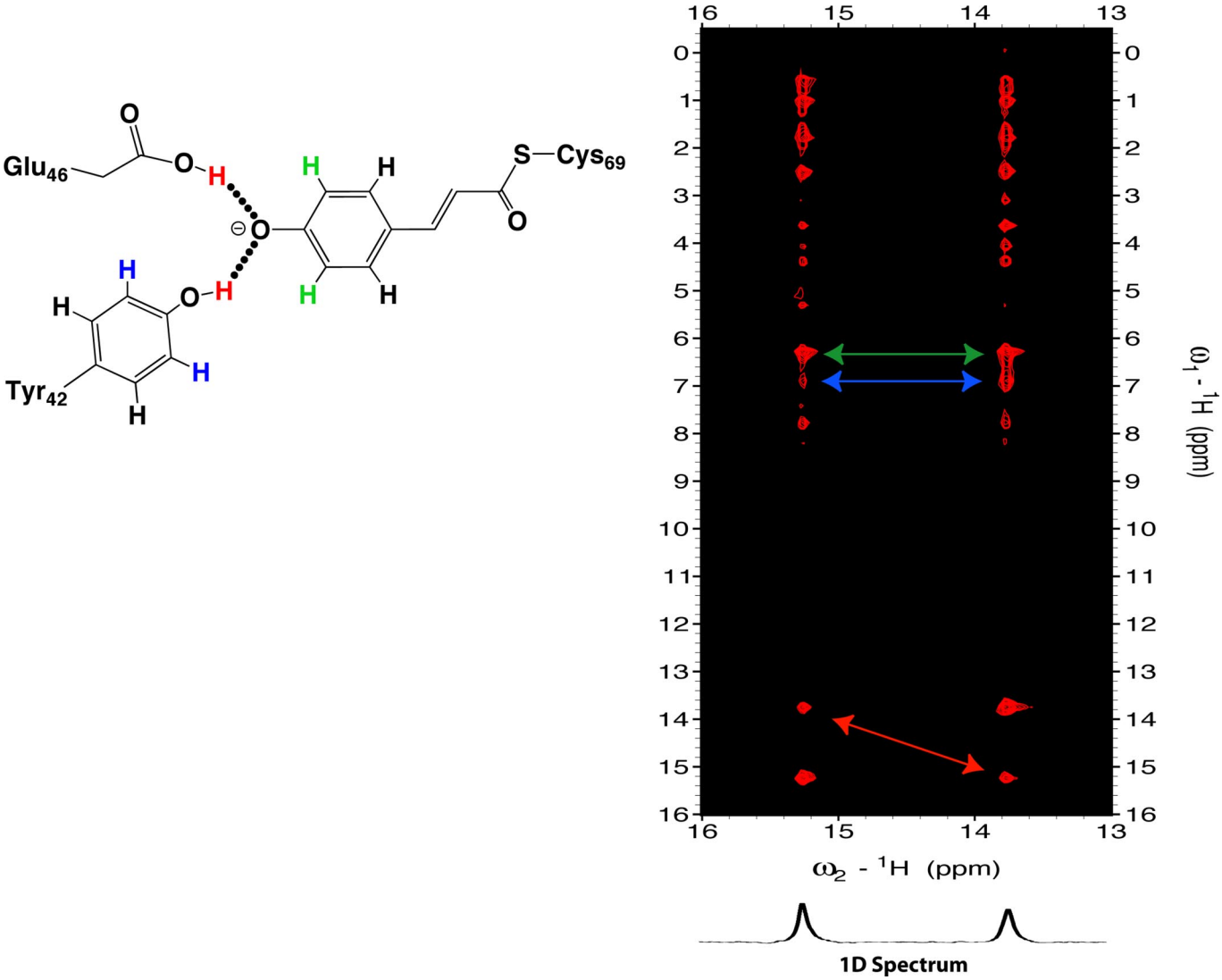

Fig. S1. ^{1}H-^{1}H NOESY spectrum of PYP acquired at 4 °C. NOE cross-peaks are detected between the 2 downfield peaks (red arrow), as expected for the near-in-space hydroxyl protons of Tyr-42 and Glu-46; between the downfield peaks and chromophore ring protons at 6.3 ppm (green arrow); and between the downfield peaks and ring protons of Tyr-42 at 6.8 ppm (blue arrow). A significantly stronger NOE to the Tyr-42 ring protons is detected for the 13.7-ppm peak than for the 15.2-ppm peak. Observed resonances were assigned using chemical shifts from the previously published NMR structure (13).

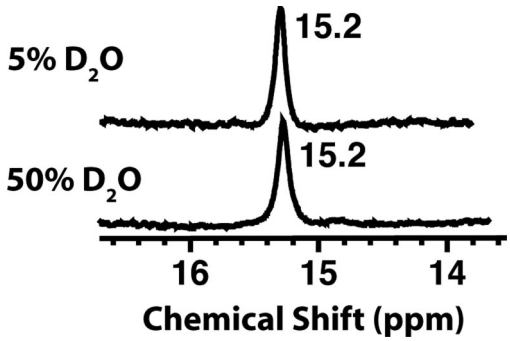

Fig. S2. ^{1}H NMR spectra of the Glu46Gln mutant of PYP in solutions containing 5% and 50% D_2O.

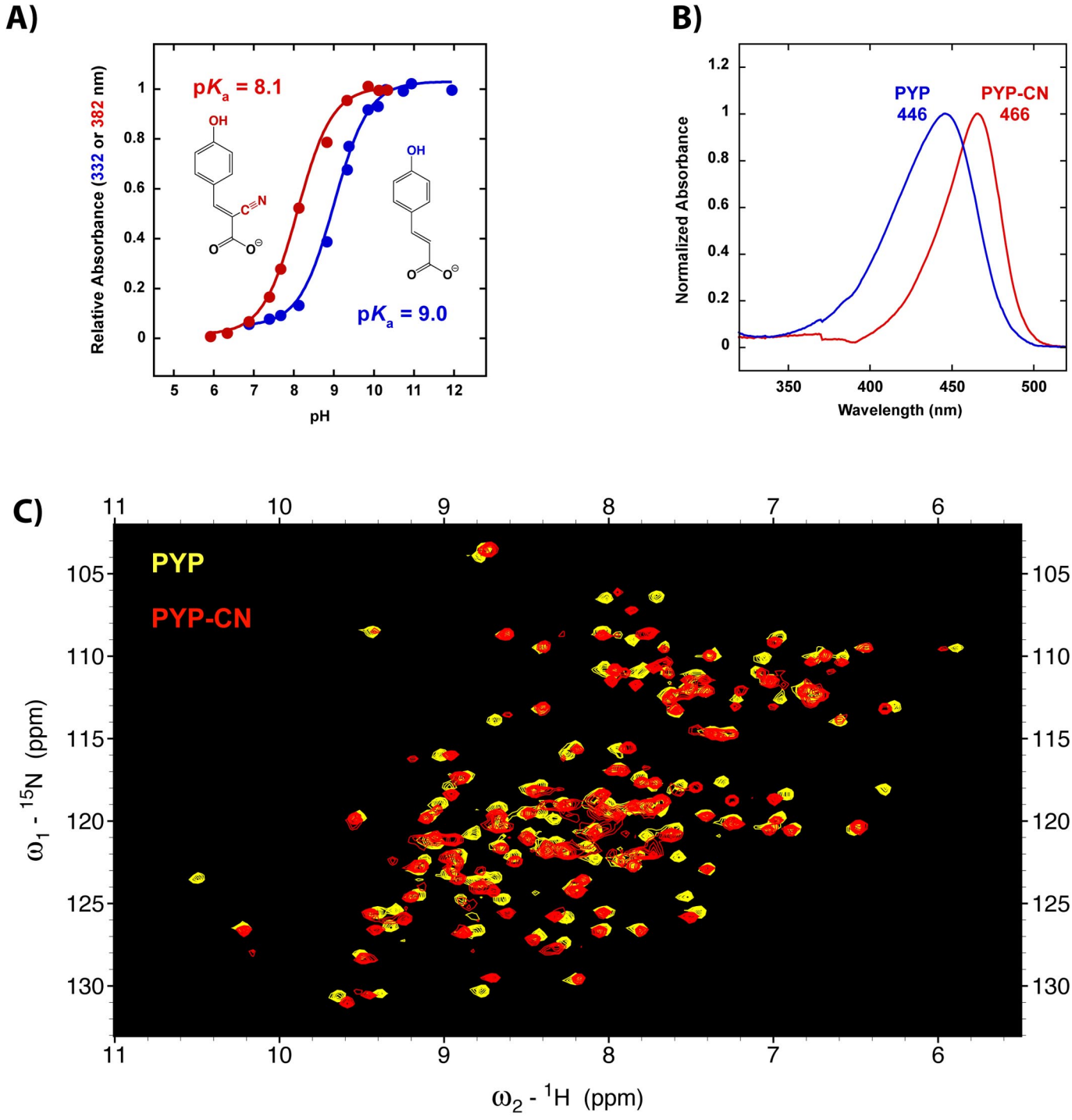

Fig. S3. Characterization of PYP-CN. (*A*) Absorbance titrations of the free *p*-coumaric acid and cyano-*p*-coumaric acid chromophores. (*B*) UV absorbance spectra of PYP and PYP-CN. (*C*) ^{1}H-^{15}N HSQC spectra of ^{15}N-labeled PYP and PYP-CN.

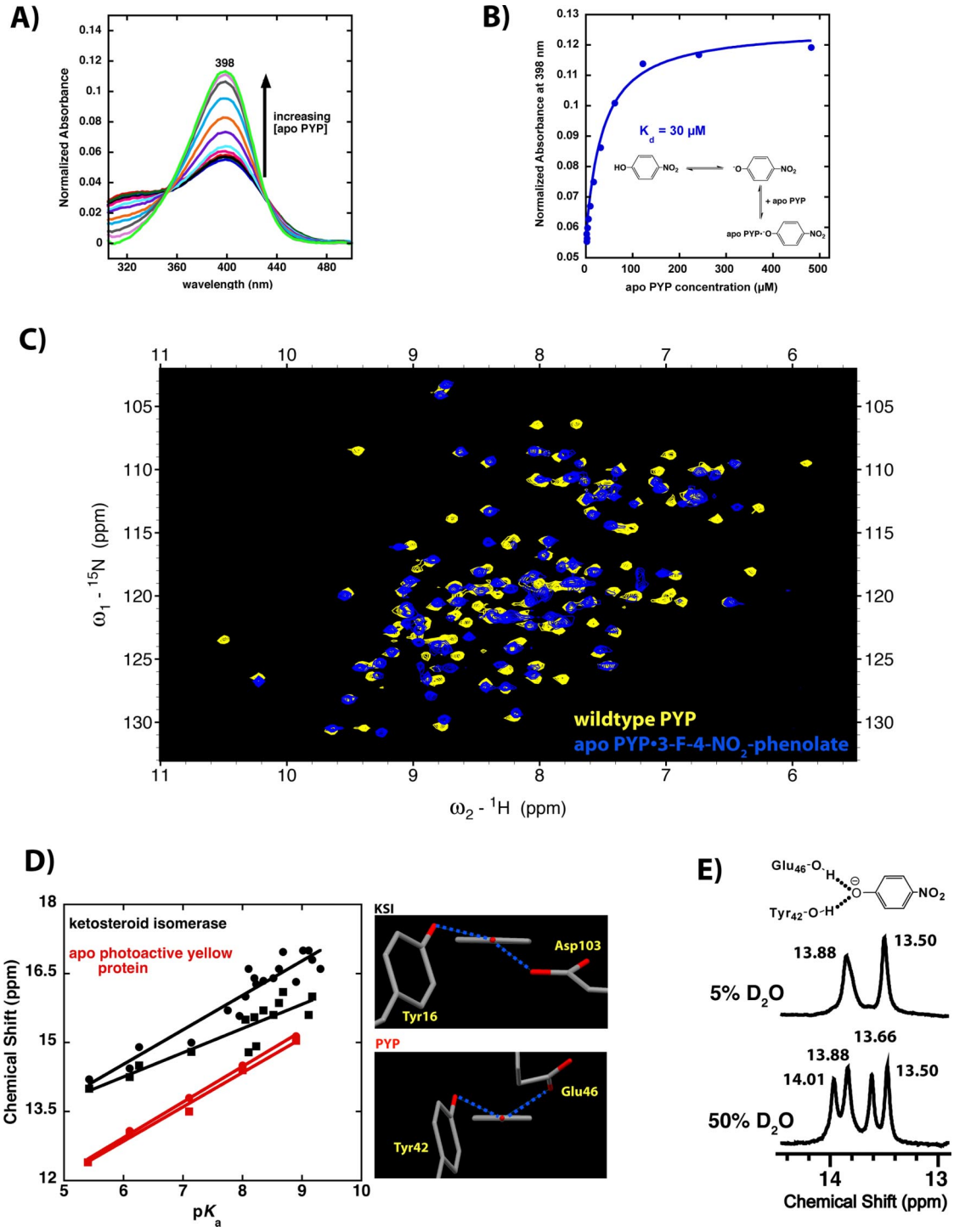

Fig. S4. Characterization of phenolate binding to apo PYP. (*A*) UV absorbance spectra of pH 7 solutions containing 5 μM 4-nitrophenol and increasing concentrations of apo PYP. (*B*) Binding of 4-nitrophenolate to apo PYP leads to a saturable increase in absorbance at 398 nm with increasing apo PYP concentration. Fitting the observed increase with a quadratic binding equation gives a dissociation constant (K_d) of 30 μM. (*C*) ^{1}H-^{15}N HSQC spectra of ^{15}N-labeled native PYP (containing the covalently attached chromophore) and apo PYP fully bound to 3-F-4-NO_2-phenolate. (*D*) Comparison of NMR data for phenolates binding to the active sites of ketosteroid isomerase (KSI) or apo PYP. KSI data are previously published (11). Structural figures compare the hydrogen bond geometries observed in the 1.25 Å resolution structure of KSI·phenol (PDB 2pzv) and the 0.82 Å resolution structure of native PYP (PDB 1nwz). (*E*) ^{1}H NMR spectra of apo PYP fully bound to 4-NO_2-phenolate in solutions containing 5% and 50% D_2O.